Slow Dielectric Relaxation of *cis*-Polyisoprene in a Polybutadiene Matrix. 2. Comparison of Experiments and Constraint Release Models

Hiroshi Watanabe,* Manabu Yamazaki, Hirotsugu Yoshida, and Tadao Kotaka

Department of Macromolecular Science, Faculty of Science, Osaka University, Toyonaka, Osaka 560, Japan

Received February 8, 1991; Revised Manuscript Received May 17, 1991

ABSTRACT: For slow dielectric relaxation of *cis*-polyisoprene (PI) entangled with a polybutadiene (PB) matrix, predictions of two types of models, the so-called CICR and CDCR models, for combined constraint release (CR) and reptation processes were compared quantitatively with the experimental data obtained in Part 1 of this series of study. In the CICR model, the rate constant of the CR process was assumed to be independent of the configuration of the PI chain, leading to the relaxation function factorized into pure CR and pure reptation functions. On the other hand, in the CDCR model, the CR process was described by configuration-dependent Rouse dynamics, and the relaxation function did not have a factorized form. The prediction of the CICR model was found to be qualitatively different from the dielectric relaxation behavior of PI chains. This suggested that the relaxation functions with the factorized form do not describe the behavior of actual entangled systems. On the other hand, reasonably good agreements with the data were found for the CDCR model *at long time scales*. This suggested the dependence on the chain configuration to be essential for the CR processes. However, *at short time scales*, agreements were poor even for the CDCR model. The limitation of the CDCR model using Rouse and reptation dynamics at *any* time scale was discussed.

I. Introduction

Binary blends composed of long and short polymer chains entangling with one another are an important model system to examine the relationship between the lifetime of entanglements and relaxation modes. The behavior of such blends, in particular, of the long-chain component, has been discussed in terms of the generalized tube model considering reptation[1] and constraint release[2-4] (CR) mechanisms. In fact, for the long chain entangled only with *much shorter* matrix chains, viscoelastic and diffusion experiments[5-11] revealed that the slow relaxation proceeds essentially via the CR mechanism that overwhelms reptation. However, those experiments also revealed that the CR dominance no longer holds as the matrix chains become long.[6,8-11] In such cases, competition of the reptation and CR mechanisms becomes important.

To further study the feature of the competition of the two mechanisms, we have examined the slow dielectric relaxation behavior of so-called *dilute* blends of *cis*-polyisoprene (PI) with polybutadiene (PB), in which a small amount of probe PI chains having (nearly) unperturbed dimensions was uniformly mixed and entangled only with matrix PB chains.[12] Two types of linear PI samples were used: One was regular PI chains that have dipoles aligned parallel in the same direction along the chain contour, and the other was those with dipole inversion at the center of the chain contour. The slow dielectric relaxation behavior of those PI chains was described in Part 1.[12] Their relaxation processes are due to fluctuation of end-to-end and/or end-to-center vectors[12-17] and referred to as the *dielectric normal mode processes*.[14]

The major findings in Part 1 were (i) significant decrease of the dielectric relaxation time τ_n and (ii) invariance of the relaxation mode distribution for the probe PI chain with decreasing matrix molecular weight M_{PB}. In addition, (iii) for the regular and dipole-inverted PI chains of (nearly) the same length, the ratio of their τ_n's was found to be insensitive to M_{PB} in spite of the significant decrease of the respective τ_n with decreasing M_{PB}.

For describing competition of reptation and constraint release (CR) mechanisms in entangled polymer systems, two types of models,[2,18,19] the so-called configuration-independent CR (CICR) and the configuration-dependent CR (CDCR) models, can be formulated, as discussed by Watanabe and Tirrell.[18] These models incorporated CR dynamics in different ways, leading to different outcomes for the dielectric relaxation behavior of the probe PI chains in the dilute blends. The experimental findings of Part 1 are useful to examine the potentiality of the two models.

In this paper, Part 2, we present results of such examination. In section III, we briefly describe the features of the CICR and CDCR models for dielectric normal mode relaxation. In section IV, we experimentally evaluate the model parameters and quantitatively compare the model predictions with the dielectric data. Some problems of the models are discussed in section V.

II. Experimental Section

Besides the narrow molecular weight distribution PI and PB samples listed in Table I of Part 1,[12] we used a PI sample (I-382) of $M_{PI} = 382 \times 10^3$, $M_w/M_n = 1.07$, and cis:trans:vinyl ratio $\simeq$ 75:20:5. The sample code number represents the molecular weight M for PB and regular PI chains without dipole inversion, and $M/2$ for a dipole-inverted PI chain, both in units of thousands. Details of dielectric measurements on PI/PB blends were described in Part 1.

Besides those measurements, linear viscoelastic measurements were made with laboratory rheometers (IR-200, Iwamoto Seisakusho; RDS-7700, Rheometrics) on homogeneous PI/PB blends in which a small amount (1.2 vol %) of long I-382 chains were mixed with B-9 or B-20 chains ($10^{-3}M_{PB}$ = 9.24 and 19.9). The time-temperature superposition was valid for the viscoelastic data. The shift factors a_T for those data were the same as a_T for the dielectric data of the PI/PB blends as well as a_T for the viscosity of bulk PBs (not of bulk PIs), as were shown in Figure 3 of Part 1. The viscoelastic data for the I-382/PB blends were used to determine parameters involved in the models examined.

0024-9297/91/2224-5372$02.50/0

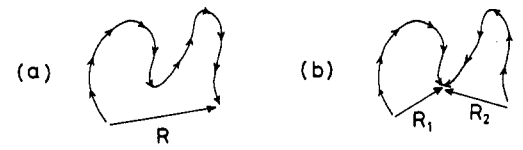

Figure 1. Schematic representation for probe (PI) chains (a) without and (b) with dipole inversion at the center of the contour.

III. Theory

1. General. In general, the complex dielectric constant $\epsilon^* = \epsilon' - i\epsilon''$ of an isotropic system is given by[20]

$$\epsilon^* - \epsilon_\infty = -\Delta\epsilon \int_0^\infty \frac{d\Phi(t)}{dt} e^{-i\omega t}\, dt \qquad (1)$$

where ω is the angular frequency, ϵ_∞ is the unrelaxed dielectric constant, $\Delta\epsilon$ is the relaxation intensity, $i^2 = -1$, and $\Phi(t)$ is the autocorrelation function of the system.

As shown in Part 1, for dilute PI/PB blends containing a small amount of probe PI chains, $\Phi(t)$ at long times is related to the motion of *individual* PI chains having (nearly) unperturbed dimensions. For regular PI chains without dipole inversion (cf. Figure 1a), we have

$$\Phi(t) = \langle \mathbf{R}(t)\cdot\mathbf{R}(0)\rangle / \langle R^2\rangle \qquad (2)$$

where $\mathbf{R}(t)$ is the end-to-end vector at time t, and $\langle ... \rangle$ represents an ensemble average at equilibrium. On the other hand, for PI chains with dipoles inverted at the center of the contour (cf. Figure 1b), we find

$$\Phi(t) = \langle \Delta\mathbf{R}(t)\cdot\Delta\mathbf{R}(0)\rangle / \langle R^2\rangle \qquad (3)$$

where $\Delta\mathbf{R}(t) = \mathbf{R}_1(t) - \mathbf{R}_2(t)$ is the difference between the two end-to-center (end-to-dipole-inversion point) vectors.

We can calculate $\Phi(t)$ for the dielectric normal mode processes of both regular and dipole-inverted PI chains (eqs 2 and 3) from a *local* correlation function $C(n,t;m)$, which represents correlation of two bond vectors at times t and 0. For a linear polymer chain composed of N bonds, $C(n,t;m)$ is defined as

$$C(n,t;m) = (1/a^2)\langle \mathbf{u}(n,t)\cdot\mathbf{u}(m,0)\rangle \qquad (0 < n, m < N) \qquad (4)$$

where $\mathbf{u}(n,t)$ is the nth bond vector at time t, and a^2 is the mean-square segment size ($=\langle u^2\rangle$). In a continuous limit (for $N \gg 1$), the *global* correlation function $\Phi(t)$ for regular PI chains (cf. eq 2) is related to $C(n,t;m)$ as

$$\Phi(t) = \frac{1}{N}\int_0^N dn \int_0^N dm\, C(n,t;m) \qquad (2')$$

Similarly, for PI chains with dipole inversion at $n = N/2$ (cf. eq 3), $\Phi(t)$ is given by

$$\Phi(t) = \frac{1}{N}\Big[\int_0^{N/2} dn \int_0^{N/2} dm + \int_{N/2}^N dn \int_{N/2}^N dm - \int_0^{N/2} dn \int_{N/2}^N dm - \int_{N/2}^N dn \int_0^{N/2} dm\Big] C(n,t;m) \qquad (3')$$

Using the (generalized tube) models described in the next section, we can calculate $C(n,t;m)$ to obtain $\Phi(t)$ (and ϵ^*; cf. eq 1) for combined reptation plus constraint release processes for the two types of PI chains.

Here, it should be noted that the local correlation function $C(n,t;m)$ for the slow *dielectric* relaxation contains first-order moments with respect to $\mathbf{u}(n,t)$ *at time* t. This feature of $C(n,t;m)$ is different from that of some other correlation functions. For example, the orientation tensor $\mathbf{S}(n,t) \propto \langle \mathbf{u}(n,t)\,\mathbf{u}(n,t)\rangle$ corresponding to viscoelastic relaxation contains second-order moments of $\mathbf{u}(n,t)$.[1] The effect of competition of constraint release and reptation is not necessarily the same for the correlation functions of different order of moments.[18] From this point of view, it is worthwhile to examine the dielectric behavior of probe PI chains in dilute blends, in addition to the viscoelastic[5-9] and diffusion[10,11] behavior of similar probes.

2. Models. For an entangled system, it is convenient to consider a primitive chain[1] (hereafter simply referred to as a chain). In the following discussion, the bond vector $\mathbf{u}$ (cf. eq 4) represents a vector connecting two neighboring entanglement points, and the segment size a corresponds to an entanglement spacing M_e. Specifically, we consider a probe (PI) chain, with and/or without dipole inversion, that is entangled *only with* matrix (PB) chains. These probe and matrix chains are composed of N_L and N_S segments, and their segmental friction coefficients are denoted by ζ_L and ζ_S, respectively. Because M_e is not necessarily the same for the probe PI and matrix PB chains and also because the PI and PB segments are chemically different, ζ_L is in general different from ζ_S.

To calculate ϵ'' for dielectric normal mode processes of a probe chain, we have to specify relaxation mechanisms of that chain. We assume that the probe chain can relax through both reptation and constraint release (CR) mechanisms. In general, the CR mechanism is considered to induce a Rouse-like motion *at long times* for the tube that confines the probe chain.[2-4] Thus (at long times) the tube is regarded as a Rouse chain composed of N_L segments with the friction coefficient ζ_t. Since the CR process is induced by the motion of the matrix chains, ζ_t increases with increasing N_S. Specifically, we use the local jump scheme of Graessley to write ζ_t as[2]

$$\zeta_t = \frac{12\Lambda(z)}{\pi^2}\zeta_S N_S^3 \qquad (5)$$

where the constant $\Lambda(z) = (\pi^2/12)^z/z$ is determined by the number z of local jump gates per entanglement segment of the probe chain.

Depending on the way the motion of the tube is incorporated, two types of models can be formulated, as discussed by Watanabe and Tirrell.[18] They derived and solved time evolution equations of the models for a function $\langle \mathbf{u}(n,t)\cdot\mathbf{R}(0)\rangle = a^2\int_0^{N_L} C(n,t;m)\, dm$ and calculated ϵ'' only for regular PI chains without dipole inversion.[18] To calculate ϵ'' for both regular and dipole-inverted PI chains (cf. eqs 1, 2', and 3'), we formulate here the two types of models for $C(n,t;m)$ (in a continuous limit).

Configuration-Independent Constraint Release (CICR) Model. In this model, the CR process is assumed to be taking place at any time uniformly throughout the chain contour. In other words, the CR process is assumed to have a rate constant $k'_{CR}(t)$ *independent* of the configuration of the probe chain trapped in the tube.

As discussed by Watanabe and Tirrell,[18] the above assumption leads to a time evolution equation for the local correlation function:

$$\frac{\partial}{\partial t}C(n,t;m) = D_c\frac{\partial^2}{\partial n^2}C(n,t;m) + k'_{CR}(t)\, C(n,t;m) \qquad (6)$$

On the right-hand side of eq 6, the first and second terms, respectively, represent changes of $C(n,t;m)$ due to reptation and CR. D_c is the curvilinear diffusion coefficient of the probe chain:

$$D_c = kT/a^2\zeta_L N_L \qquad (7)$$

The rate constant $k'_{CR}(t)$ for the dielectric CR process is written as[18]

$$k'_{CR}(t) = \frac{1}{\nu_{CR}(t)}\frac{d\nu_{CR}(t)}{dt} \qquad (8)$$

with

$$\nu_{CR}(t) = \sum_{q=\text{odd}} \frac{8}{q^2\pi^2} \exp[-D_t\lambda_q{}^2 t] \quad (\text{for } N_L \gg 1) \quad (9)$$

Here, the tube segment mobility, D_t, is defined as

$$D_t = \frac{3kT}{a^2\zeta_t} \quad (\propto N_S{}^{-3}) \qquad \lambda_q = \frac{q\pi}{N_L} \quad (q = 1, 2, ...) \quad (10)$$

The probe PI chains in the dilute PI/PB blends examined in Part 1 are in a (nearly) unperturbed state.[12] For such a probe chain with large N_L, the initial condition for $C(n,t;m)$ may be written as[21]

$$C(n,0;m) = \frac{2}{N_L} \sum_{p=1}^{N_L} \sin(\lambda_p n) \sin(\lambda_p m) \quad (11)$$

The boundary condition is

$$C(n,t;m) = 0 \quad \text{for } n, m = 0, N \quad (12)$$

which represents random orientation at chain ends. With these conditions, we can solve eq 6 to obtain

$$C(n,t;m) = \nu_{CR}(t)\frac{2}{N_L} \sum_{p=1}^{N_L} \sin(\lambda_p n) \sin(\lambda_p m) \exp[-D_c\lambda_p{}^2 t] \quad (13)$$

From eqs 2′, 3′, and 13, we finally obtain the global correlation function $\Phi(t)$ and the *dielectrically observed* longest relaxation time τ_1. For regular PI chains without dipole inversion, we have

$$\Phi(t) = \nu_{CR}(t)\,\nu_{rep}(t) = \sum_{p=\text{odd}} \sum_{q=\text{odd}} \frac{8}{p^2\pi^2}\frac{8}{q^2\pi^2} \exp\left[-\left(\frac{q^2}{\tau_{CR}} + \frac{p^2}{\tau_{rep}}\right)t\right] \quad (14a)$$

and

$$\tau_1 = \frac{1}{(1/\tau_{CR}) + (1/\tau_{rep})} \quad (15a)$$

For dipole-inverted PI chains, we find

$$\Phi(t) = \nu_{CR}(t)\,\nu_{rep}(4t) = \sum_{p=\text{odd}} \sum_{q=\text{odd}} \frac{8}{p^2\pi^2}\frac{8}{q^2\pi^2} \exp\left[-\left(\frac{q^2}{\tau_{CR}} + \frac{4p^2}{\tau_{rep}}\right)t\right] \quad (14b)$$

and

$$\tau_1 = \frac{1}{(1/\tau_{CR}) + (4/\tau_{rep})} \quad (15b)$$

In eqs 14a and 14b, $\nu_{rep}(t)$ denotes the reduced reptation function:

$$\nu_{rep}(t) = \sum_{p=\text{odd}} \frac{8}{p^2\pi^2} \exp[-D_c\lambda_p{}^2 t] \quad (16)$$

The characteristic times for the CR and reptation processes involved in eqs 14a–15b are given by

$$\tau_{CR} = N_L{}^2/D_t\pi^2 \quad (17)$$

and

$$\tau_{rep} = N_L{}^2/D_c\pi^2 \quad (18)$$

As seen in eqs 14a and 14b, the correlation function $\Phi(t)$ deduced from the CICR model is *factorized* into the functions for pure CR (ν_{CR}) and pure reptation (ν_{rep}) processes. Thus, in this model, changes in the relative magnitudes of D_t and D_c or, more specifically, changes in N_S and N_L induce changes not only in the relaxation times τ_1 (eqs 15a and 15b) but also in the mode distribution of $\Phi(t)$ and ϵ^*. This is one of the most prominent features of the CICR model for the dielectric normal mode processes.

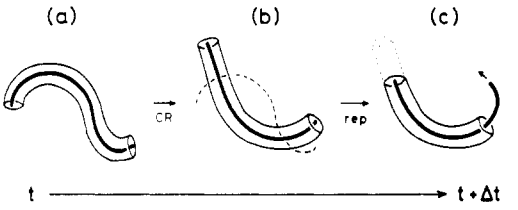

Figure 2. Schematic representation for changes of the configuration of a probe chain due to a combined constraint release plus reptation mechanism. During a short period of time Δt, the tube first deforms (from a to b), and then the probe chain (solid line) reptates along this deformed tube (b to c).

For regular and dipole-inverted PI chains of the same length N_L, the global motion itself is the same but the dielectric τ_1 is different. Concerning this point, we note from eqs 15a and 15b that the ratio of τ_1's predicted by the CICR model for the two types of probe chains changes with N_S and N_L. This is another prominent feature of the CICR model.

In some models[2,3,19] for combined CR plus reptation processes, an *independence* of CR and reptation is assumed in a sense that the probability of survival of initial memory for the combined process is given by a product of the probabilities for *pure* CR and *pure* reptation processes. Because $\Phi(t)$ represents this probability for dielectric normal mode relaxation, the above assumption directly leads to the factorized form of $\Phi(t)$, as predicted also by the CICR model (cf. eqs 14a and 14b). The equivalence of a class of models[2,3,19] assuming the *independence in the above sense* and the CICR model was discussed by Watanabe and Tirrell.[18]

Configuration-Dependent Constraint Release (CDCR) Model. If the CR process proceeds through a Rouse mechanism as usually considered, the rate constant k'_{CR} (cf. eq 6) of that process should be dependent on the chain configuration, i.e., on both n and t. From this argument, Watanabe and Tirrell[18] pointed out a problem of the CICR model and proposed another model referred to as the configuration-dependent constraint release (CDCR) model.

The CDCR model assumes that CR and reptation processes successively take place during a short period of time Δt (cf. Figure 2) and uses eigenfunction expansion to describe changes in the chain configuration. In general, competition of the two processes formulated in this way leads to changes in the eigenvalue problem for local relaxation functions.

For the time evolution of $C(n,t;m)$ with the boundary condition, eq 12, the eigenfunctions are the same for Rouse (CR) and reptation dynamics and given by $\sin(\lambda_p n)$ ($p = 1, 2, ..., N_L$; $\lambda_p = p\pi/N_L$). Using these eigenfunctions, we formulate here the CDCR model for $C(n,t;m)$. First at time t (Figure 2a), $C(n,t;m) = (1/a^2)\langle \mathbf{u}(n,t)\cdot\mathbf{u}(m,0)\rangle$ is expanded with respect to the Rouse eigenfunctions:

$$C(n,t;m) = \sum_{p=1}^{N_L} A_p(t;m) \sin(\lambda_p n) \quad (19)$$

Here, $A_p(t;m)$ is the amplitude of the eigenfunction of the

order p at time t and evaluated by

$$A_p(t;m) = \frac{2}{N_L}\int_0^{N_L} dn\, C(n,t;m) \sin(\lambda_p n) \quad (20)$$

During the CR step (from Figure 2a to 2b), $A_p(t;m)$ decays according to Rouse (CR) dynamics by a factor $\exp(-D_t\lambda_p^2\Delta t)$, with D_t being the tube segment mobility. Since the Rouse and reptation eigenfunctions for $C(n,t;m)$ are identical, the amplitude for the latter at the end of the CR step (Figure 2b) is also given by $A_p(t;m)\exp(-D_t\lambda_p^2\Delta t)$. During the reptation step (from Figure 2b to 2c), this amplitude further decays by a factor $\exp(-D_c\lambda_p^2\Delta t)$, with D_c being the curvilinear diffusion coefficient. Thus, at time $t + \Delta t$ (Figure 2c), the configuration of the probe chain is described by

$$C(n,t+\Delta t;m) = \sum_{p=1}^{N_L} A_p(t;m)\exp[-(D_t + D_c)\lambda_p^2\Delta t]\sin(\lambda_p n) \quad (21)$$

From eqs 19–21 with $\Delta t \to 0$, we obtain a time evolution equation:

$$\frac{\partial}{\partial t}C(n,t;m) = [D_t + D_c]\frac{\partial^2}{\partial n^2}C(n,t;m) \quad (22)$$

Here, we note a prominent feature of the CDCR model for $C(n,t;m)$. As seen from eqs 19 and 21, decay of the amplitude $A_p(t;m)$ for the Rouse (CR) eigenfunction of the order p is affected only by the reptation eigenfunction of the *same* order, and vice versa, because of the coincidence of these two eigenfunctions for $C(n,t;m)$. In other words, the coupling between slow reptation and CR modes is not disturbed by the fast modes.

With eqs 11 and 12, we can solve eq 22 to find

$$C(n,t;m) = \frac{2}{N_L}\sum_{p=1}^{N_L}\sin(\lambda_p n)\sin(\lambda_p m)\exp[-(D_t + D_c)\lambda_p^2 t] \quad (23)$$

From eqs 2′, 3′, and 23, we finally obtain the global correlation function $\Phi(t)$ and the dielectric relaxation time τ_1. For regular PI chains, we have

$$\Phi(t) = \sum_{p=\text{odd}} \frac{8}{p^2\pi^2}\exp\left[-p^2\left(\frac{1}{\tau_{CR}} + \frac{1}{\tau_{rep}}\right)t\right] \quad (24a)$$

and

$$\tau_1 = \frac{1}{(1/\tau_{CR}) + (1/\tau_{rep})} \quad (25a)$$

For dipole-inverted PI chains, we find

$$\Phi(t) = \sum_{p=\text{odd}} \frac{8}{p^2\pi^2}\exp\left[-4p^2\left(\frac{1}{\tau_{CR}} + \frac{1}{\tau_{rep}}\right)t\right] \quad (24b)$$

and

$$\tau_1 = \frac{1}{4}\frac{1}{(1/\tau_{CR}) + (1/\tau_{rep})} \quad (25b)$$

In eqs 24a–25b, the characteristic times, τ_{CR} and τ_{rep}, are the same as those given in eqs 17 and 18, respectively.

The features of the CDCR model (eqs 24a–25b) are essentially different from those of the CICR model (eqs 14a–15b). First, the CDCR model *does not* predict a factorized form of $\Phi(t)$. Instead, it predicts $\Phi(t)$ (and ϵ^*) to have a universal mode distribution independent of N_S and N_L. In addition, it predicts that the ratio of the dielectric τ_1's of the dipole-inverted and regular PI chains *of the same length* (N_L) is just 1/4 and dependent on *neither* N_S *nor* N_L (cf. eqs 25a and 25b). These features of the CDCR model are due to the coincidence of the reptation and Rouse eigenfunctions for $C(n,t;m)$.

IV. Results

1. Model Parameters. The CICR and CDCR models contain the same set of fundamental parameters; the number N_L of entanglement segments per probe chain, the curvilinear diffusion coefficient of the probe chain D_c ($\propto 1/\zeta_L N_L$), and the tube segment mobility D_t ($\propto 1/\zeta_S N_S^3$). To *separately* determine these parameters, we have to know the entanglement spacing $M_e^{I/B}$ ($=M_{PI}/N_L$) and segmental friction coefficient ζ_L for *probe PI chains placed in PB matrices*. As discussed in Part 1,[12] it is difficult to evaluate $M_e^{I/B}$ and ζ_L without introducing any assumptions.

However, as can be seen in eqs 14a–15b and 24a–25b, we need only two quantities, τ_{CR} (CR time; eq 17) and τ_{rep} (reptation time; eq 18), to compare the models with experiments. The τ_{CR} and τ_{rep} are written in terms of *combinations* of the fundamental parameters, N_L, D_c, and D_t, and conveniently cast into the following forms:

$$\tau_{CR} = \frac{N_L^2}{D_t\pi^2} = t^\circ_{CR} M_{PB}^3 M_{PI}^2 \quad (17')$$

$$\tau_{rep} = \frac{N_L^2}{D_c\pi^2} = t^\circ_{rep} M_{PI}^3 \quad (18')$$

Here, t°_{CR} and t°_{rep} are constants *independent* of the molecular weights of the probe PI (M_{PI}) and matrix PB (M_{PB}) chains. Thus, through some adequate experiments, we can determine the values of t°_{CR} and t°_{rep} without explicitly knowing $M_e^{I/B}$ and ζ_L.

Determination of t°_{CR}. We can determine t°_{CR} from the slow relaxation behavior of *long* probe PI chains entangled only with *much shorter* PB matrix chains. In such a *CR-dominant regime* (where $\tau_{CR} \ll \tau_{rep}$), the slow relaxation of the probe PI chains took place at low frequencies not manageable with the dielectric spectrometer available to us. Thus, we have determined t°_{CR} from viscoelastic measurements that well covered the frequencies for the slow relaxation.

Figure 3 shows master curves of storage moduli G' at 40 °C for homogeneous PI/PB blends containing 1.2 vol % of I-382 chains that entangle only with much shorter matrix B-9 or B-20 chains. In the frequency range examined, G' values of the blends were much larger than G' values of the matrix and thus attributable to the I-382 chains involved.

For the slow viscoelastic relaxation in the CR-dominant regime, both the CICR and CDCR models (with the Doi–Edwards initial condition[1,2]) lead to the *same* G' for the probe PI chains:[18]

$$G'(\omega;M_{PI}) = \frac{4\rho\phi_{PI}RT}{5M_{PI}}\sum_p \frac{[\omega\tau_{CR}/2p^2]^2}{1 + [\omega\tau_{CR}/2p^2]^2} \quad (26)$$

Here, ρ is the density of the blends and R is the gas constant. For I-382/PB blends with small ϕ_{PI} (=1.2 vol %), we replaced ρ by the density of bulk PB (=0.90 g/cm^3).[22] Note that the longest relaxation time for G' in the CR-dominant regime is half of τ_{CR} for $\phi(t)$ and ϵ^*.

For a quantitative comparison of the observed and calculated G' shown in Figure 3, we made a correction for a small but finite molecular weight distribution (MWD) of I-382 (M_w/M_n = 1.07). To this end, we used a MWD

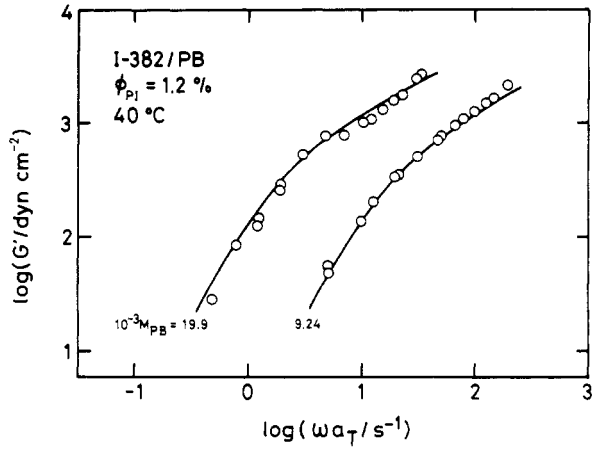

Figure 3. Frequency dependence of the storage moduli G' at 40 °C for PI/PB blends containing ϕ_{PI} = 1.2 vol % of I-382 chains (with $10^{-3}M_{PI}$ = 382). The matrix B-9 and B-20 chains (with $10^{-3}M_{PB}$ = 9.24 and 19.9) are much shorter than the I-382 chain. The solid curves indicate the G' calculated from the CDCR and CICR models for pure CR (Rouse) processes with a parameter $t°_{CR} = 8.94 \times 10^{-25}$ s. A small MWD of I-382 was incorporated in the calculation through eq 27.

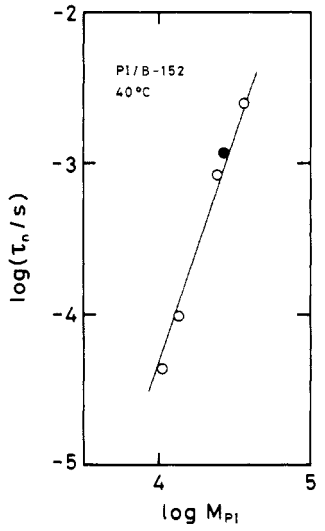

Figure 4. M_{PI} dependence of dielectric relaxation times τ_n of dilute PI chains in the B-152 matrix at 40 °C. For the 2(I-13) chain with dipole inversion, $4\tau_n$ is plotted against M_{PI} (filled circle). The solid line denotes the prediction of the CICR and CDCR models with a parameter $t°_{rep} = 5.03 \times 10^{-17}$ s.

function of I-382 determined by gel permeation chromatography.[12] We divided the MWD function into 5 and/or 10 fractions and evaluated the molecular weight M_{PI}^i and weight fraction w_i of the ith fraction (i = 1, 2, ..., f; f = 5 or 10). Using these M_{PI}^i and w_i, we calculated G' as

$$G' = \sum_i w_i G'(\omega;M_{PI}^i) \qquad (27)$$

Here, $G'(\omega;M_{PI}^i)$ is the storage modulus given by eq 26 with M_{PI} being replaced by M_{PI}^i. The G' curves calculated from the MWD function with 5 and 10 fractions were indistinguishable. The results are indicated with the solid curves in Figure 3. As seen there, the data for the I-382/PB blends are well described by the two models with[23]

$$t°_{CR} = 8.94 \times 10^{-25}\ \text{s} \quad (40\ °C) \qquad (28)$$

Determination of $t°_{rep}$. We can determine $t°_{rep}$ from the dielectric relaxation time τ_1 of probe PI chains entangled only with *much longer* matrix PB chains. For such cases where reptation is considered to be dominant ($\tau_{rep} \ll \tau_{CR}$), the CICR and CDCR models give the *same* τ_1 (cf. eqs 15 and 25):

$$\tau_1 = \tau_{rep} = t°_{rep}M_{PI}^3, \quad \text{for PI without dipole inversion} \qquad (29a)$$

$$\tau_1 = \tau_{rep}/4 = (t°_{rep}/4)M_{PI}^3, \quad \text{for PI with dipole inversion} \qquad (29b)$$

In Part 1,[12] dielectric relaxation times τ_n were determined from the location of maxima of the ϵ'' curves for five probe PI chains (with $10^{-3}M_{PI} \le 35.4$) entangled with much longer PB matrix chains (with $10^{-3}M_{PB}$ = 152). The dielectric relaxation mode distribution was narrow and universal for those PI chains (cf. Figure 8), and the ϵ'' peaks corresponded well to the terminal zones. Thus, we do not distinguish τ_n and τ_1 to evaluate $t°_{rep}$ from the τ_n data. Figure 4 shows the M_{PI} dependence of τ_n. For the dipole-inverted 2(I-13) chain, $4\tau_n$ is plotted against M_{PI} (the filled circle), as suggested from eqs 29a and 29b. As seen in Figure 4, τ_n of PI chains in much longer matrix chains are reasonably well described by the two models (eq 29) with

$$t°_{rep} = 5.03 \times 10^{-17}\ \text{s} \quad (40\ °C) \qquad (30)$$

2. Comparison of Experiments and Models. Using the parameters $t°_{CR}$ and $t°_{rep}$ (eqs 28 and 30) evaluated in the previous section, we made a quantitative comparison of the data and model predictions.

Table I summarizes the ratio $\tau_{CR}/\tau_{rep} = t°_{CR}M_{PB}^3/t°_{rep}M_{PI}$ (cf. eqs 17′ and 18′) for the probe PI chains subjected to dielectric measurements. As seen in Table I, $\tau_{CR} \gg \tau_{rep}$ for all PI chains in the longest B-152 matrix. This indicates that reptation is dominant for the PI chains in that matrix, satisfying the prerequisite for the evaluation of $t°_{rep}$ from the data in Figure 4. On the other hand, in the shortest B-9 matrix the ratio is in the vicinity of unity, meaning that the CR and reptation mechanisms have comparable contributions to the dielectric relaxation of the PI chains examined.

For the I-382/PB blends examined in Figure 3, we also evaluated the ratio of the CR and reptation times from $t°_{CR}$ and $t°_{rep}$ (eqs 28 and 30). The viscoelastic CR time is given by $\tau_{CR}/2$ (cf. eq 26). The $(\tau_{CR}/2)/\tau_{rep}$ ratios were 0.18 and 0.018 for the I-382 chains in the B-20 and B-9 matrices, respectively. These small ratios, in particular,

Table I
τ_{CR}/τ_{rep} Ratio for PI Chains in Various PB Matrices

$10^{-3}M_{PI}$	τ_{CR}/τ_{rep}[a]
$M_{PB} = 9.24 \times 10^3$	
13.4	1.05
23.8	0.59
26.2[b]	0.54
35.4	0.40
$M_{PB} = 19.9 \times 10^3$	
13.4	10.5
23.8	5.89
26.2[b]	5.35
$M_{PB} = 152 \times 10^3$	
13.4	4660
23.8	2620
26.2[b]	2380
35.4	1760

[a] Calculated from $t°_{CR}$ and $t°_{rep}$ (cf. eqs 17′, 18′, 28, and 30). [b] With dipole inversion.

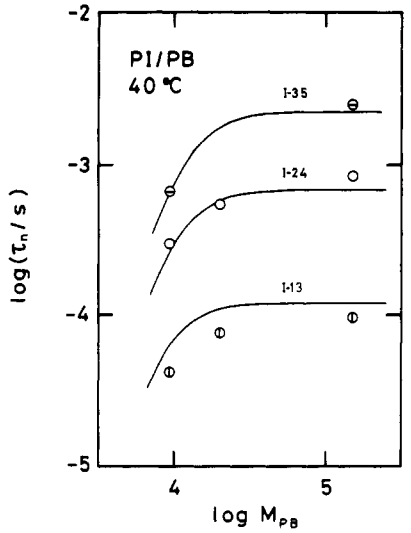

Figure 5. M_{PB} dependence of the dielectric relaxation time of the probe PI chains without dipole inversion in dilute PI/PB blends at 40 °C. The solid curves indicate the prediction of the CICR and CDCR models (eqs 15a and 25a).

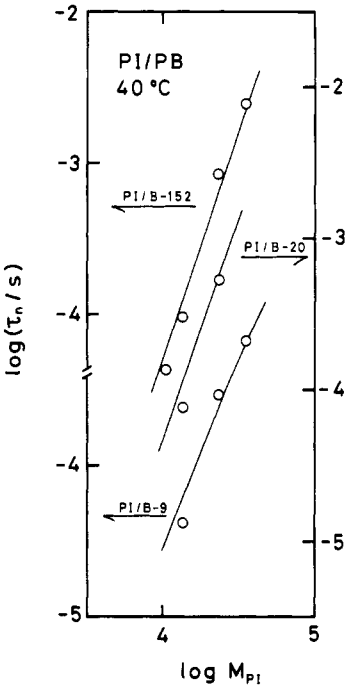

Figure 6. M_{PI} dependence of the dielectric relaxation time of the probe PI chains without dipole inversion in dilute PI/PB blends at 40 °C. The solid curves indicate the prediction of the CICR and CDCR models (eqs 15a and 25a).

the latter, indicate the CR dominance for the relaxation of probe I-382 chains in the blends, satisfying the prerequisite for the evaluation of t°_{CR} from the data in Figure 3.

Figures 5 and 6, respectively, show the dependence of dielectric relaxation time τ_n of regular PI chains without dipole inversion on matrix and probe molecular weights M_{PB} and M_{PI}. The τ_1 ($\simeq\tau_n$) values predicted by the CICR and CDCR models are the same (eqs 15a and 25a) and are indicated with the solid curves. As can be seen in Figures 5 and 6, the τ_n data are reasonably well described by the two models.[25]

To distinguish the features of the two models for the regular PI chains, we compared the dielectric relaxation mode distribution. For PI chains without molecular weight distribution (MWD), the CDCR model (eq 24a) does not

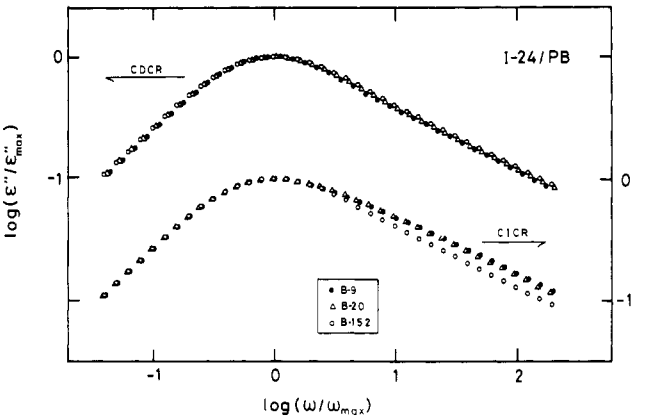

Figure 7. Comparison of the dielectric relaxation mode distribution calculated by the CDCR (top) and CICR (bottom) models for the probe I-24 chain in various PB matrices as indicated. A small MWD of I-24 was incorporated in the calculation.

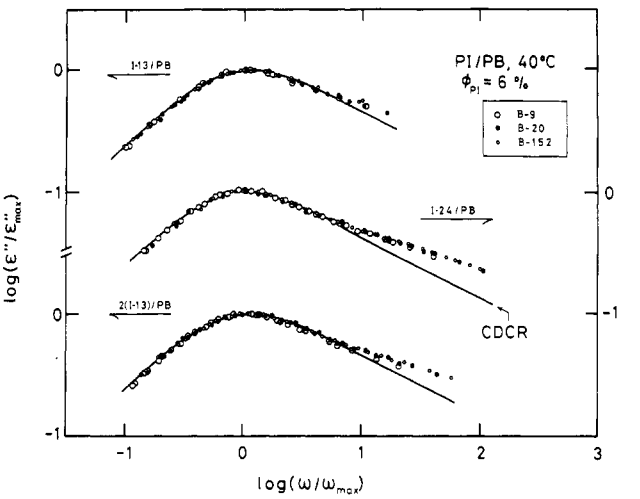

Figure 8. Comparison of the dielectric relaxation mode distribution of the probe PI chains in various PB matrices. The solid curves indicate the prediction of the CDCR model considering MWD.

but the CICR model (eq 14a) does predict changes in the mode distribution due to changes in M_{PB} and M_{PI}. The PI chains used in this study had a small but finite MWD. Thus, as we did for G' (cf. eq 27), we used the MWD functions of the PI chains to calculate the ϵ'' curves for the two models. The curves calculated for I-24 (M_w/M_n = 1.05) are shown in Figure 7 as an example.

In Figure 7, we note that the small MWD hardly affects the universality of the mode distribution deduced from the CDCR model for I-24. This was the case for all PI chains (with $M_w/M_n \leq 1.06$) examined. On the other hand, the CICR model leads to a nonuniversal mode distribution as clearly seen in Figure 7. We already found in Part 1[12] that slow dielectric mode distributions of probe PI chains are universal irrespective of the probe and matrix molecular weights (cf. Figure 8 also). This experimental result supports the CDCR model but not the CICR model.

Figure 8 compares the universal relaxation mode distribution of probe PI chains[12] (circles) with the prediction of the CDCR model (corrected for small MWD; solid curves). Reasonably good agreements are observed for the terminal relaxation behavior at low frequencies $\omega \leq 10\omega_{max}$ ($=10/\tau_n$). However, at higher ω, we see significant differences between the data and model prediction. As seen in eq 24, the values of τ_{CR} and τ_{rep} as well as their M_L and M_S dependences do not affect the shape of the ϵ''

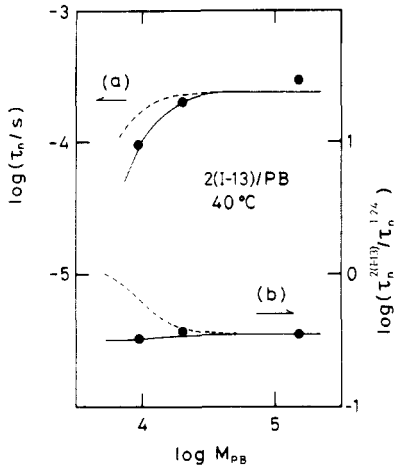

Figure 9. (a) M_{PB} dependence of the dielectric relaxation time of the probe 2(I-13) chain in PB matrices at 40 °C. (b) M_{PB} dependence of the ratio of τ_n's of the 2(I-13) and I-24 chains in PB matrices at 40 °C. 2(I-13) and I-24 have nearly the same M_{PI} but the latter has no inversion of dipoles. The solid and dashed curves indicate the predictions of the CDCR and CICR models, respectively. In (b), a slight decrease of the $\tau_n^{2(I-13)}/\tau_n^{I-24}$ ratio with decreasing M_{PB} predicted by the CDCR model (solid curve) is due to a small difference in M_{PI} of the two PI chains.

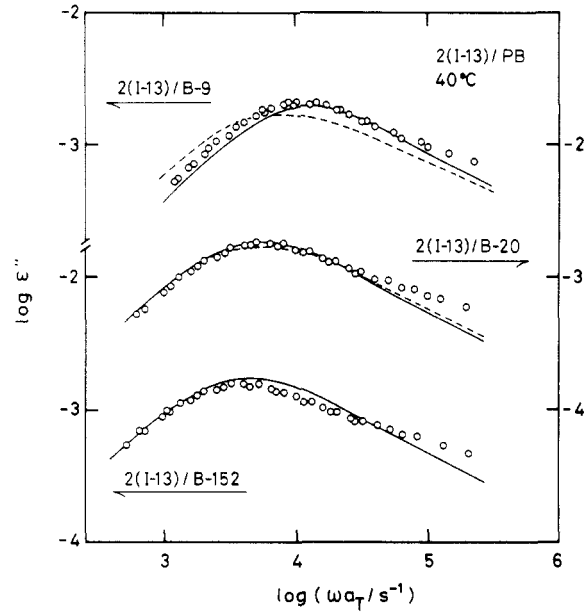

Figure 10. Dielectric loss curves of the probe 2(I-13) chain (ϕ_{PI} = 6 vol %) in various PB matrices as indicated. The solid and dashed curves indicate the predictions of the CDCR and CICR models, respectively.

curves deduced from the CDCR model. Thus, the poor agreements at high ω found in Figure 8 are essential and must reflect a problem(s) involved in the CDCR model of the present form (eqs 19–22). This problem(s) is discussed in section V.

Figure 9 compares the data (circles) and model predictions (solid and dashed curves) for the dielectric relaxation time τ_n of the dipole-inverted 2(I-13) chain. Part a shows τ_n of that PI chain plotted against the matrix molecular weight M_{PB}. In part b, we examine the M_{PB} dependence of the ratio of τ_n's of 2(I-13) and I-24, both having nearly the same M_{PI} but the latter having no inversion of dipoles. For 2(I-13), the τ_n values predicted by the CICR and CDCR models are not the same (cf. eqs 15b and 25b). As can be seen in Figure 9, in particular in part b, agreements with the data are much better for the CDCR model (solid curves) than for the CICR model (dashed curves).

Figure 10 compares the observed and calculated ϵ'' curves for 2(I-13) in various matrices as indicated. As was done in Figures 3, 7, and 8, a correction for the small MWD of 2(I-13) (M_w/M_n = 1.06) was incorporated in the calculation.[26] For the theoretical ϵ'' curves, the relaxation intensity $\Delta\epsilon$ (cf. eq 1) was determined in such a way that the best agreement between the observed and calculated curves was obtained at low $\omega \lesssim 10\omega_{max}$ for all PI/B-152 blends examined in Part 1.[12] (In those high-M_{PB} blends, reptation was dominant and the predictions of the CICR and CDCR models were indistinguishable for all PI chains examined.) As can be seen in Figure 10, the agreement with the data for the 2(I-13)/B-9 blend (with small M_{PB}) is much better for the CDCR model (solid curve) than for the CICR model (dashed curve).

V. Discussion

As seen in Figures 7–10, the prediction of the CICR model is qualitatively different from the data for probe PI chains in PB matrices. Thus, the relaxation functions with the factorized form (cf. eq 14) *do not* describe the dielectric behavior of probe PI chains. Dependence on configuration of the probe chain seems to be essential for CR processes. On the other hand, for the CDCR model, we have found reasonably good agreements with the data at *long* time scales (cf. Figures 7–10). Thus, low-order Rouse and reptation eigenfunctions incorporated in the CDCR model (cf. eqs 19–21) seem to be valid to describe the terminal relaxation of the probe PI chains.

However, even for the CDCR model, we have found poor agreements at *short* time scales (cf. Figure 8). The model in the present form is essentially a model good only for terminal relaxation, because of the following limitations of reptation and Rouse dynamics used in the model. In Figure 8, we see that the CDCR model poorly describes ϵ'' at high ω even in a reptation-dominant regime (in the B-152 matrix). Reptation dynamics underestimates fast dielectric modes, possibly because reptation is already a coarse-grained molecular motion realizable only at long time scales.

We also note another problem for the CDCR model. As can be seen in eq 19, the model uses Rouse modes as the CR modes *at any time scale* (for any mode-order p). This inevitably results in the following problem. As seen in Figure 8, the probe PI chains in various PB matrices exhibit a universal behavior and the CDCR model always underestimates their ϵ'' at high ω to the same extent irrespective of M_{PI} and M_{PB} (irrespective of the relative contributions of the CR and reptation mechanisms). This suggests that the Rouse dynamics used in the model underestimates the dielectric modes at *short* time scales to the same extent as the reptation dynamics does. (The short time scale discussed here is still long enough as compared to the time scale of segmental mode discussed in Part 1.[12]) Even for *nonentangled* bulk PI to which the Rouse model should be most adequately applicable, the model was found to underestimate ϵ'' at high ω.[15,27] Thus, the validity of Rouse dynamics is essentially limited to long time scales. The limitation of Rouse dynamics for description of real CR processes will be further examined in our next paper.[28]

Finally, we add a comment on why the CDCR model reasonably well describes ϵ'' at long time scales in spite of the invalidity of Rouse and reptation dynamics at short time scales. In the model, coupling between *slow* Rouse and reptation modes is not disturbed by the fast modes (cf. eqs 19 and 21). This feature enables the model to

describe ϵ'' at long time scales in terms of *only* low-order Rouse and reptation eigenfunctions, those being valid to describe the terminal relaxation (cf. Figures 3, 4, and 8–10).

VI. Conclusion

Predictions of the two models, the so-called CICR and CDCR models, for combined constraint release (CR) and reptation processes have been compared quantitatively with the slow dielectric relaxation behavior of two types of probe PI chains entangled with matrix PB chains. The prediction of the CICR model was found to be qualitatively different from the experimental results. We thus conclude that the CICR model and resulting relaxation functions with the factorized form (cf. eq 14) *do not* adequately describe dynamic behavior in real systems.

On the other hand, for the CDCR model, we have found reasonably good agreements with the data although limited at *long* time scales. Thus, the dependence on the configuration of the probe chain appears to be essential for CR processes. However, at *short* time scales, the model poorly described the dielectric relaxation behavior of probe PI, because of limitations of reptation and Rouse (CR) dynamics used in the model. The CDCR model in the present form is essentially a model good only for terminal relaxation.

References and Notes

(1) Doi, M.; Edwards, S. F. *The Theory of Polymer Dynamics*; Clarendon: Oxford, 1986.
(2) Graessley, W. W. *Adv. Polym. Sci.* **1982**, *47*, 67.
(3) Klein, J. *Macromolecules* **1978**, *11*, 852.
(4) Daoud, M.; de Gennes, P.-G. *J. Polym. Sci., Polym. Phys. Ed.* **1979**, *17*, 1971.
(5) Watanabe, H.; Kotaka, T. *Macromolecules* **1984**, *17*, 2316.
(6) Watanabe, H.; Sakamoto, T.; Kotaka, T. *Macromolecules* **1985**, *18*, 1008, 1436.
(7) Watanabe, H.; Kotaka, T. *Macromolecules* **1986**, *19*, 2520.
(8) Watanabe, H.; Kotaka, T. *Macromolecules* **1987**, *20*, 530.
(9) Watanabe, H.; Yoshida, H.; Kotaka, T. *Macromolecules* **1988**, *21*, 2175.
(10) Green, P. F.; Mills, P. J.; Palmstrøm, C. J.; Mayer, J. W.; Kramer, E. J. *Phys. Rev. Lett.* **1984**, *53*, 2145.
(11) Green, P. F.; Kramer, E. J. *Macromolecules* **1986**, *19*, 1108.
(12) Watanabe, H.; Yamazaki, M.; Yoshida, H.; Adachi, K.; Kotaka, T. *Macromolecules*, preceding paper in this issue.
(13) Stockmayer, W. H. *Pure Appl. Chem.* **1967**, *15*, 539.
(14) Adachi, K.; Kotaka, T. *Macromolecules* **1984**, *17*, 120.
(15) Imanishi, Y.; Adachi, K.; Kotaka, T. *J. Chem. Phys.* **1988**, *89*, 7585.
(16) Adachi, K.; Itoh, S.; Nishi, I.; Kotaka, T. *Macromolecules* **1990**, *23*, 2554.
(17) Yoshida, H.; Watanabe, H.; Adachi, K.; Kotaka, T. *Macromolecules* **1991**, *24*, 2981.
(18) Watanabe, H.; Tirrell, M. *Macromolecules* **1989**, *22*, 927.
(19) (a) Rubinstein, M.; Helfand, E.; Pearson, D. S. *Macromolecules* **1987**, *20*, 822. (b) Doi, M.; Graessley, W. W.; Helfand, E.; Pearson, D. S. *Macromolecules* **1987**, *20*, 1900.
(20) Cole, R. H. *J. Chem. Phys.* **1965**, *42*, 637.
(21) For large N_L, eq 11 is essentially the same as an initial condition, $C(n,0;m) = 1$ for $|n - m| < {}^1/_2$ and $C(n,0;m) = 0$ for $|n - m| > {}^1/_2$.
(22) Stephenes, H. L. In *Polymer Handbook*, 3rd ed.; Brandrup, J., Immergut, E. H. Eds.; Wiley: New York, 1989; Chapter V.
(23) It is interesting to examine the local jump gate number z (cf. eq 5) estimated from the t°_{CR} value (eq 28), although we do not use this z value in the present work. If we *assume* that the entanglement segment size, a, is the same for the probe PI and matrix PB chains, we may use the Graessley–Edwards scheme[24] for M_e ($\propto a^{1/2}$) to estimate $M_e^{I/B}$ for PI chains in PB matrices. From eqs 5, 10, 17′, and 28 together with N_L ($=M_{PI}/M_e^{I/B}$) estimated in this way, we obtained $z \simeq 4.4$. This z value is physically reasonable, suggesting that t°_{CR} (eq 28) has been evaluated on a sound basis.
(24) Graessley, W. W.; Edwards, S. F. *Polymer* **1981**, *122*, 1329.
(25) Adachi and co-workers[16] *assumed* an adequate z value (cf. eq 5) and found reasonably good agreements between the τ_n for narrow MWD bulk PI (without dipole inversion) and the prediction of the Graessley model[2] that is equivalent to the CICR model discussed in this paper. In addition, they found that the dielectric mode distributions of low-M PI chains (with $M_{PI}/M_e \simeq 3$ and 6) are the *same* in monodisperse systems (where CR should have significant contribution) and in high-M PI matrices (with negligible CR contribution). For regular PI chains, the CICR and CDCR models predict the same τ_n (eqs 15a and 25a) but different mode distributions: The former predicts differences between the distributions of PI in the monodisperse systems and in high-M matrices (eq 14a), while the latter does not (eq 24a). Thus, the above findings of Adachi and co-workers[16] support the CDCR model rather than the CICR model.
(26) Strictly speaking, we also have to consider a distribution of location of dipole inversion point along the chain contour.[17] However, for the narrow MWD 2(I-13) chain, that distribution was small and hardly affected the universality of the calculated ϵ'' curves. Thus, we neglected the correction for that distribution in the present calculation.
(27) Imanishi, Y. M.S. Dissertation, Osaka University, 1987.
(28) Watanabe, H.; Yamazaki, M.; Yoshida, H.; Kotaka, T. *Macromolecules*, in press.

Registry No. PI (homopolymer), 9003-31-0; PB (homopolymer), 9003-17-2.